ELSEVIER

Chemical Geology 216 (2005) 113–131

CHEMICAL GEOLOGY
INCLUDING
ISOTOPE GEOSCIENCE

www.elsevier.com/locate/chemgeo

# Depositional and paleohydrogeological controls on the distribution of organic matter and other reactive reductants in aquifer sediments

N. Hartog[a,*], J. Griffioen[b], P.F. van Bergen[a,1]

[a]*Department of Geochemistry, Faculty of Earth Sciences, Utrecht University, P.O. Box 80021, 3508 TA Utrecht, The Netherlands*
[b]*TNO Netherlands Institute of Applied Geosciences TNO, P.O. Box 80019, 3508 TA Utrecht, The Netherlands*

Received 2 March 2004; accepted 2 November 2004

**Abstract**

The reactivity of sedimentary reductants is the main control for the natural attenuation of common groundwater contaminants, such as nitrate or chlorinated hydrocarbons. Middle Miocene to Late Pleistocene (0.01–20 My old) aquifer sands of marine, fluvial, fluvio-glacial and aeolian origin were characterized to determine the control of sediment depositional environment, sediment age and paleohydrology on the distribution and reactivity of sedimentary reductants. In addition to the variability in the molecular composition of sedimentary organic matter (SOM), the reduction reactivity of these sediments was determined. Oxygen consumption and carbon dioxide production during sediment incubations indicated that SOM, pyrite and ferrous iron-bearing carbonates were the main reductants. Bulk $\delta^{13}C_{org}$-values (~25‰) indicated that terrestrial higher land plants were the main precursor of SOM, regardless of sediment origin. However, pyrolysis-GC/MS analysis showed that SOM in the marine Tertiary sands contained lignin with preserved side-chains, while in the Pleistocene fluvial and fluvio-aeolian sediments, highly degraded lignin and recalcitrant macromolecular aliphatic structures dominated SOM, indicative of aerobic degradation. The higher dynamics of these terrestrial depositional environments as compared with their marine counterpart, likely allows for increased oxygen exposure times and thus more intense aerobic degradation of SOM. The aquifer sediment that fills a large erosional valley created during the Saale ice-age, likely consists of fluvio-glacially reworked marine Tertiary sediments, as supported by carbonate isotopic evidence. The more degraded status and decreased reactivity of SOM in this sediment than in its precursor, is likely due to the increased oxygen exposure during dynamic fluvio-glacial reworking. Despite the highly degraded nature of SOM and the absence of pyrite in the Pleistocene fluvial and fluvio-aeolian sediments, oxygen consumption rates were high during the incubation of sediments from the shallowest part of the aquifer. A reactive ferroan carbonate phase was inferred as the main source of oxidant demand in shallow fluvial and aeolian sands. Depleted oxygen and carbon isotopes indicated that this phase was groundwater derived.

* Corresponding author. Current address: Department of Earth Sciences, University of Waterloo, Waterloo, ON, Canada N2L 3G1. Tel.: +1 519 888 4567x7003; fax: +1 519 883 0220.

*E-mail address:* nhartog@uwaterloo.ca (N. Hartog).

[1] Current address: Shell Global Solutions International, Amsterdam, The Netherlands.


doi:10.1016/j.chemgeo.2004.11.006

Aerobic degradation during sediment deposition appears to control the molecular composition and reactivity of SOM in aquifer sediments and to affect the potential of subsequent diagenetic pyrite formation. In addition, (paleo)hydrological conditions may result in the accumulation of a ferrous iron-bearing carbonate phase precipitated during the exfiltration of Fe(II)-containing anoxic groundwater.


*Keywords:* Kerogen; Sedimentary organic matter; Pyrite; Ferrous iron; Oxygen reduction; Pyrolysis; Carbonate isotopes

## 1. Introduction

The fate of several common groundwater contaminants, such as nitrate, chromate or chlorinated hydrocarbons depends on the reduction capacity present in the groundwater system, as their solubility or toxicity alters upon reduction (Blowes, 2002; Bradley et al., 1998; Postma et al., 1991; Smith and Duff, 1988). For most sedimentary aquifers, reduced species associated with the sediment phase represent the predominant pool of reduction capacity as compared to dissolved reductants (Amirbahman et al., 1998; Barcelona and Holm, 1991; Heron and Christensen, 1995; Pedersen et al., 1991). Of the reductants found in aquifer sediments, sedimentary organic matter (SOM) is most ubiquitous and numerous groundwater field studies have identified the coupling of SOM oxidation with the reduction of oxygen, nitrate, iron(III) and sulfate (Jakobsen and Postma, 1994; Lovley et al., 1990; Morris et al., 1988; Puckett and Cowdery, 2002; Smith and Duff, 1988). Furthermore, it has been demonstrated that reduction rates observed in the field are limited by the availability of SOM (Bradley et al., 1995; Desimone and Howes, 1996; Hill et al., 2000; Jakobsen and Postma, 1994; Pfenning and McMahon, 1996; Starr et al., 1996). Recently, Hartog et al. (2004) focused on the factors that control the reactivity of SOM in aquifers by comparing the molecular composition of SOM in aquifer sediment of fluvio-glacial and marine origin. Molecular indicators on the oxidation state of SOM in these sediments could be related to its degradability during sediment incubations.

SOM plays a central role in the redox chemistry of groundwater systems. Not only may SOM act as a reactive reductant, but also anaerobic degradation of SOM drives the diagenetic formation of reactive iron(II)-, manganese(II)- or sulfide-bearing minerals in aquifers (Jakobsen and Postma, 1999; Magaritz and Luzier, 1985). These secondary reductants, such as pyrite ($FeS_2$) or siderite ($FeCO_3$), may also react with introduced oxidants. Pyrite oxidation coupled to oxygen and nitrate reduction is frequently reported in field studies (Kelly, 1997; Molenat et al., 2002; Pauwels et al., 2001; Postma et al., 1991), while experimental studies on isolated reductants have shown that siderite and other Fe(II)-bearing minerals, such as detrital silicates, are also potentially important (Hofstetter et al., 2003; Lee and Batchelor, 2003; Postma, 1990; Weber et al., 2001).

Depending on the provenance, depositional environment and diagenetic history of the aquifer sediments, a range of sedimentary reductants may thus be competing for oxidants. For example, Böhlke and Denver (1995) concluded that the combined oxidation of SOM, glauconite and pyrite were responsible for denitrification observed in a coastal plain aquifer. Moreover, differences in the relative contribution of co-oxidizing sedimentary reductants during the experimental determination of sediment reduction capacities have been related to variations in the geological sediment origin within a simple aquifer (Hartog et al., 2002). In an integrated approach, the current study explores the relationships between the geological history of aquifer sediments, the types of sedimentary reductants present and their reactivity. To gain insight in the governing factors a wide range of Middle Miocene to Late Pleistocene (0.01–20 My old) aquifer sediments with marine, fluvial, fluvio-glacial and aeolian origins were investigated. Our main objectives were to elucidate (1) the variability in the molecular composition of SOM in controlling the reduction capacities of aquifers and (2) the role of sediment depositional environment, sediment age and paleohydrology on the distribution and reactivity of sedimentary reductants.

## 2. Site description

### 2.1. Geohydrology

The study area is located in the eastern part of The Netherlands near drinking water production site t Klooster (Fig. 1). Here, sediments of Pleistocene and Miocene origin form a thick unconsolidated sequence of sandy deposits, locally separated by clay layers to form interconnected aquifers. The hydrogeological base is formed by Miocene marine clays of the Breda Formation at 100–120 m below surface (Figs. 1 and 2). Within the aquifer system studied, the glauconitic Breda and Oosterhout Formations form the oldest deposits and are of marine and near-shore origin. The continuous uplift of the hinterland in the East caused the coastal zone to gradually shift to the west. Towards the end of the Tertiary, the area was situated in the coastal zone, with an influx of continental sands (Scheemda Formation). Fluvial sediments were deposited from the early Pleistocene onward. First, these fluvial deposits had a Baltic origin, but during the Middle Pleistocene Rhine-Meuse sediments (e.g., the Urk Formation) became dominant. Glacial and fluvio-

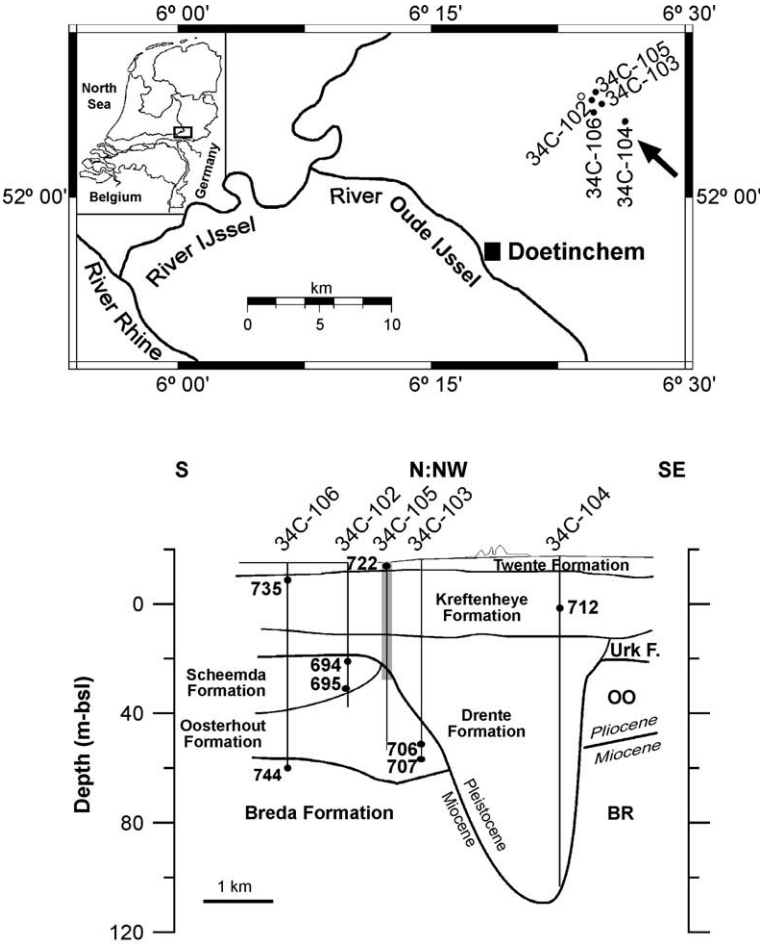


Fig. 1. Location of study area and geological profile. (A) The study area in the eastern part of The Netherlands, showing (1) the location of the cores used (filled circles), (2) location of the drinking water production site (open circle), (3) general groundwater flow direction (arrow). (B) Profile shows the main geological formations within the cores studied. Depth is indicated in meters below sea level (m-bs). Shaded area represents the depth range of samples that were selected for incubation experiments (Fig. 8). Numbers refer to the samples selected for Py-GC/MS analyses (Table 1).

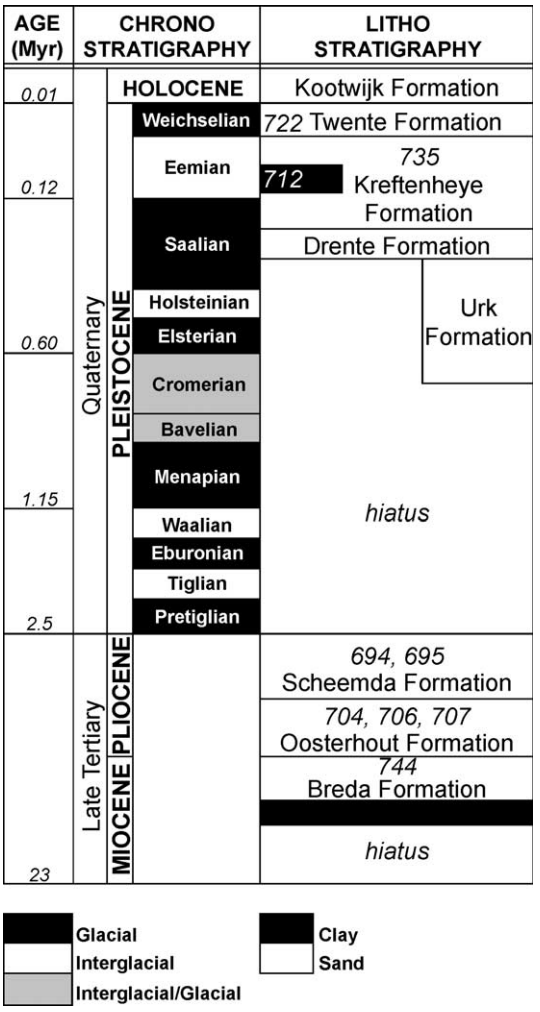


Fig. 2. Late Tertiary and Quaternary chronostratigraphy and lithostratigraphic units for the area studied (simplified after van den Berg et al. (2000). Age indications after Funnell (1996) and van den Berg et al. (2000). Numbers refer to samples selected for Py-GC/MS analyses (Table 1).

glacial sediments (Drente Formation) were deposited during the Saalian, when push moraines were formed and severe fluvio-glacial erosion occurred. Locally, the infill of deeply incised valleys (core 34-C104, Fig. 1) largely consists of eroded older strata. Fluvial sedimentation (Kreftenheye Formation) returned at the start of the Eemian interglacial. Additionally, local fluvio-aeolian sediments (Twente Formation) were deposited during the Weichselian periglacial period. Holocene aeolian deposits of the Kootwijk Formation are locally present (van den Berg et al., 2000).

Groundwater levels are 2–6 m below surface (m-bs) and occur in the Twente and Kreftenheye deposits. Large-scale abstraction of phreatic groundwater (5 $mm^3$ $year^{-1}$) for drinking water production and intensified drainage have resulted in the disappearance of local seepage areas. At the site studied (Fig. 1), groundwater flow direction is NW (Uffink and Römkens, 2001).

### 2.2. Hydrochemistry

The groundwater chemistry of the area studied is well documented (Griffioen, 2001; van Beek and Vogelaar, 1998). Dissolved oxygen is depleted within the first 2 m below surface, leaving the largest part of the sedimentary sequence presently under anoxic conditions. Locally, shallow groundwater is influenced by agricultural activities as illustrated by nitrate concentrations up to 200 mg/l at mini-screen well WP4 (core location: 34C-105, Fig. 1A). Denitrification takes place within the first 15 m below surface, while sulfate disappears in the depth interval between 30 and 55 m-bs. Locally, methane is observed at depths great than 15–30 m-bs (Griffioen, 2001; van Beek and Vogelaar, 1998).

## 3. Materials and methods

### 3.1. Sediment sampling

Sediment samples were selected from various cores around the drinking water production site ‘t Klooster (Fig. 1). Sediment cores were obtained in 40-cm-long stainless steel tubing with a 65-mm inner diameter, using a hollow stem auger. Sediment samples collected were stored in glass bottles at 8 °C until they were sieved into a 0–2000-μm fraction. The >2000-μm fraction (<5 wt.%) was discarded. Fractions were stove-dried (40 °C) and subsamples were taken for isotope analysis, sedimentary organic matter isolation and batch incubation experiments.

### 3.2. Sediment analysis

#### 3.2.1. SOM: isolation and molecular characterization

Samples were selected from the major geological formations within the aquifer system studied

(Figs. 1 and 2). All selected samples were sandy, except one sample taken from a clay layer in the Kreftenheye Formation. No samples were selected from the sediment-filled erosion valley as they were characterized previously in a study in which the effect of fluvio-glacial sediment reworking on molecular SOM composition was assessed (Hartog et al., 2004).

To concentrate the organic matter present, samples were treated with excess 10% HCl to remove carbonates and settled overnight, after which the samples were centrifuged at 2200 rpm for 7 min and the supernatant was decanted. Samples were then treated with excess 38% HF to dissolve the silicate mineral matrix, shaken at 250 rpm for 2 h, after which the samples were centrifuged at 2200 rpm for 7 min and the supernatant was decanted. Then, the samples were washed three times with distilled water by centrifugation and decantation as described above. Subsequently, the HCl and HF procedure as described above was repeated. Finally, samples were treated with 30% HCl to remove any potential fluoride gels and were washed as described above until the samples were diluted to pH 7. Isolates were freeze-dried and weighed. The HCl/HF treatment removed 81–99% of the mineral matrix, and likely resulted in the loss of some organic compounds, but studies have indicated that it does not significantly affect the bulk composition of the organic matter isolated (Sanchez-Monedero et al., 2002; Schmidt et al., 1997). The dried isolates were stored in glass at 8 °C in the dark until analysis by pyrolysis-gas chromatography/mass spectrometry (Py-GC/MS).

Curie-point Py-GC/MS was used to characterize SOM at a molecular level. The organic matter isolates were pressed onto a ferromagnetic wire with a Curie temperature of 610 °C. Py-GC/MS analyses were carried out using a Hewlett-Packard 5890 gas chromatograph (GC) equipped with a FOM-3LX unit for pyrolysis. The GC was interfaced to a VG Autospec Ultima mass spectrometer operated at 70 eV with a mass range of *m/z* 50–800 and a cycle time of 1.7 s (resolution 1000). The GC, equipped with a cryogenic unit, was programmed from 0 °C (5 min) to 300 °C (10 min) at a rate of 3 °C/min. Separation was achieved using a fused silica capillary column (25 m×0.32 mm) coated with CP Sil-5CB (film thickness 0.4 μm). Helium was used as a carrier gas.

### 3.2.2. Carbon and oxygen isotope analysis

Inorganic carbon was removed before analysis by shaking the sample for 24 h in 1 M HCl. Stable carbon isotope analyses of bulk SOM ($\delta^{13}C_{org}$) were obtained by on-line combustion of decalcified samples using a Fisons Instruments NA 1500 Elemental Analyser (EA) coupled via a ConFlo II interface to a Finningan MAT Delta Plus isotope ratio mass spectrometer (IRMS). Laboratory standards NBS-21 and NBS-22 were processed to check for systematic errors of $\delta^{13}C_{org}$ analysis. Overall analytical errors were better than ±0.1‰ (2$\sigma$). Anomalously heavy $\delta^{13}C_{org}$-values (>−10‰) were recorded for some carbonate-rich samples. To remove recalcitrant carbonates, samples were re-exposed to acid for 2 weeks with dilute HCl (0.4 M) together with control samples. This additional acid treatment did not have a significant effect on the $\delta^{13}C_{org}$ as indicated by the unaltered isotopic value of the control samples.

Oxygen and carbon isotopic ratios of carbonates ($\delta^{18}O_{carb}$, $\delta^{13}C_{carb}$) were measured on freeze-dried sediment samples. Samples were transferred to an automated carbonate preparation unit (IsoCarb). The samples were transferred into glass reaction tubes that were evacuated for 14 h. Subsequently, 100% phosphoric acid was added at 25 °C under high vacuum for 6 h. The $CO_2$ released was cryogenically separated from other gases and isotope values were measured on an isotope ratio mass spectrometer (VG SIRA 24). Values are reported relative to the PeeDee Belemnite in standard $\delta$ notation. Precision for $\delta^{18}O$ and for $\delta^{13}C$ measurements was better than 0.5‰.

### 3.2.3. Incubation experiments

Sediment samples with a dry weight of 34–41 g were incubated with 50 ml of vitamin and trace elements solution (Hartog et al., 2002), under dark conditions for 7.5 days. The reaction chambers (100-ml bottle, Duran) were connected to the closed circuit of a respirometer (Micro-Oxymax, Columbus Instruments). Water-saturated gases were used to prevent evaporation in the reaction chambers. Oxygen ($p_{O_2}=10^{-0.68\pm0.002}$ atm) and carbon dioxide ($p_{CO_2}=10^{-3.51\pm0.11}$ atm) levels in the headspaces were kept at atmospheric conditions at 25 °C (±1 °C). The $O_2$ consumption and $CO_2$ production were measured every 3 h with an analytical precision of ±3 nmol using an infrared sensor and an oxygen battery (fuel

cell), respectively. The reaction chambers were shaken (100 rpm) on a shaking table to ensure a well-mixed chemical system and prevent gas transfer limitations.

Directly after incubation, pH was measured with a standard pH meter (Orion) and alkalinity was determined by acid titration. Dissolved cations and sulfate were analyzed using ICP-AES (Perkin-Elmer ICP-optima 3000). Speciation calculations were performed using PHREEQC (Parkhurst and Appelo, 1999). The saturation index (SI) is defined as the logarithmic value of the ratio between the ion activity product and the solubility constant for a given mineral.

## 4. Results

First, the molecular composition and carbon isotope composition of SOM in aquifer sediments from various geological formations is presented. Then, the variation in and relationships between carbon and oxygen isotopic values of the carbonate phase are shown. Finally, the oxygen consumption and the relationship with carbon dioxide production during incubation of aquifer sediments from core 34C-105 are investigated.

### 4.1. Sediment chemistry

#### 4.1.1. Molecular composition of SOM

Curie point pyrolysis-GC/MS was used as a qualitative method to characterize the molecular composition of SOM in selected aquifer sediments (Table 1). Evaporate/pyrolysate mixtures all revealed the presence of relatively abundant aromatic compounds, homologous series of *n*-alk-1-enes and *n*-alkanes and $C_{16}$ and $C_{18}$ fatty acids (25–26, Fig. 3). These compounds dominate the chromatograms of the pyrolysates of the sandy Twente (722, Fig. 3) and Kreftenheye (735) samples. In contrast, phenolic and guaiacyl-lignin derived compounds with minor contributions from fatty acids (25–26) and branched hydrocarbons (e.g., 23) dominate the evaporate/pyrolysate mixtures of the marine and coastal sands and the fluvial Kreftenheye clay sample (712).

Alkane/alkene doublets form the dominant aliphatic contribution in all samples (Fig. 3). Alkenes dominate the alkane counterparts in the short-chain range (C<20). However, long-chain alkanes become more pronounced with increasing carbon number. Especially between $C_{25}$ and $C_{29}$, the alkanes dominate their alkene counterparts. For these alkanes, a distinct odd-over-even predominance is observed, as illustrated by the mass chromatograms *m/z* 55+57 (Fig. 4).

All samples reveal the presence of guaiacyl-derived lignin units with various degrees of side-chain degradation as illustrated by the mass chromatograms *m/z* 124+138+150+152+164+166. In the pyrolysate/evaporate mixtures of the Kreftenheye sand (735) and Twente (722, Fig. 3) samples, only a minor signal from guaiacol (peak 11 in Fig. 3, peak **I** in Fig. 5) was observed. All other samples showed guaiacyl components with various side-chain lengths (Fig. 5) ranging from methylguaiacol (**II**) to the eugenol isomers (**V**, **VII**, **VIII**). Guaiacol was the dominant lignin derivative in the Scheemda samples, while 4-vinyl-2-methoxyphenol (**IV**) and methylguaiacol were dominant in the Oosterhout and Breda samples. In

Table 1
Bulk characteristics of the sediment samples used for Py-GC/MS analysis

| Core | Sample code | Formation | Depth (m-bs) | Depth (m-NAP) | TOC (wt.%) | Carbonate (wt.%) | Fe (wt.%) | S (wt.%) | Mn (wt.%) | $\delta^{18}O_{carb}$ (‰ PDB) | $\delta^{13}C_{carb}$ (‰ PDB) | $\delta^{13}C_{org}$ (‰ PDB) |
|---|---|---|---|---|---|---|---|---|---|---|---|---|
| 34C-102 | 694 | SC | 39.2 | −23.1 | 0.14 | 0.62 | 4.70 | 0.15 | 0.02 | NA | NA | −24.9 |
| 34C-102 | 695 | SC | 49.2 | −33.1 | 0.36 | 6.25 | 5.18 | 0.18 | 0.03 | 0.91 | 0.94 | −25.8 |
| 34C-103 | 706 | OO | 68.2 | −52.1 | 0.40 | 1.79 | 3.27 | 0.16 | 0.01 | 1.58 | 1.08 | −25.0 |
| 34C-103 | 707 | OO | 74.2 | −58.1 | 0.31 | 0.80 | 4.15 | 0.1 | 0.01 | 1.97 | −0.15 | −24.7 |
| 34C-104 | 712 | KR | 20.2 | −2.7 | 0.76 | 6.74 | 2.25 | 0.1 | 0.07 | −4.76 | −0.74 | −26.7 |
| 34C-105 | 722 | TW | 3.2 | 12.0 | 0.19 | 5.42 | 1.32 | ND | 0.03 | −3.10 | −7.96 | −24.4 |
| 34C-106 | 735 | KR | 10.2 | 5.9 | 0.2 | 10.27 | 1.31 | ND | 0.04 | −2.41 | −7.30 | −24.3 |
| 34C-106 | 744 | BR | 76.2 | −60.1 | 0.24 | 0.73 | 3.85 | 0.16 | 0.01 | 2.42 | 1.98 | −26.7 |

NA: not analyzed. ND: not detected. TOC (Total Organic Carbon), Carbonate, Fe, Mn and S data from van Beek and Vogelaar (1998).

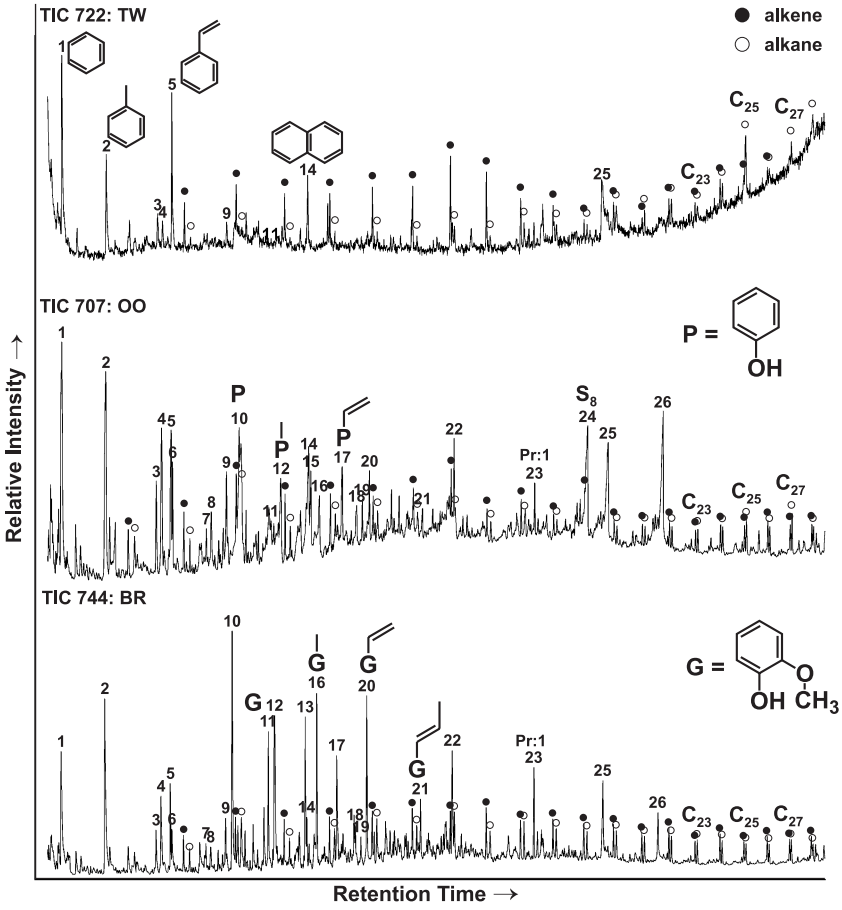


Fig. 3. Total ion current traces of the evaporate/pyrolysate mixtures of SOM samples from the Twente (722), Oosterhout (707) and Breda (744) Formation. Key: (1) Benzene, (2) Toluene, (3) $C_2$-Alkylbenzene (AB), (4) $C_2$-AB, (5) Styrene, (6) $C_2$-AB, (7–9) $C_3$-AB, (10) Phenol, (11) Guaiacol, (12) Methylphenol, (13) $C_4$-AB, (14) Naphthalene, (15) $C_4$-AB, (16) Methylguaiacol, (17) Vinylphenol, (18–19) Methylnaphthalene, (20) Vinylguaiacol, (21) *trans*-Isoeugenol, (22) 3,5-di(*tert*-butyl)phenol (contaminant), (23) Prist-1-ene, (24) Elemental sulfur ($S_8$), (25) $C_{16}$-Fatty Acid, (26) $C_{18}$-Fatty Acid, ○=alkane, ●=alkene.

these samples also the eugenol isomers were more pronounced. The guaiacyl side chains were remarkably well preserved in the Kreftenheye clay (712, Fig. 5) sample when compared with the Kreftenheye sand (735) sample. The oxidized lignin derivatives 4-formyl-2-methoxyphenol (**VI**) and 4-acetyl-2-methoxyphenol (**IX**) were observed in all samples except 722 and 735.

Parallel to the guaiacyl-derived lignin components, pentacyclic triterpenoid hydrocarbons of bacterial hopanoid origin showed side-chain degradation features, as illustrated by the mass chromatograms *m/z* 191 (not shown). Hopanoid distributions range from $C_{27}$ to $C_{33}$. No hopanoid-derived compounds were observed in the Twente (722) and Kreftenheye (735) samples.

### *4.1.2. Organic carbon and carbonate isotope chemistry*

The $\delta^{13}C_{org}$-values of 28 SOM samples ranged between −23‰ and −27‰ (average −25.1‰ ±1.1). No consistent variation over depth or with various geological formations was observed (Table 1).

All seven marine sediment samples (Oosterhout and Breda Formation) show $\delta^{18}O_{carb}$ and $\delta^{13}C_{carb}$ values close to the reference value of zero (Table 1, Fig. 6). Similarly, all six samples from the fluvioglacial Drente Formation show only small (−0.5‰ to

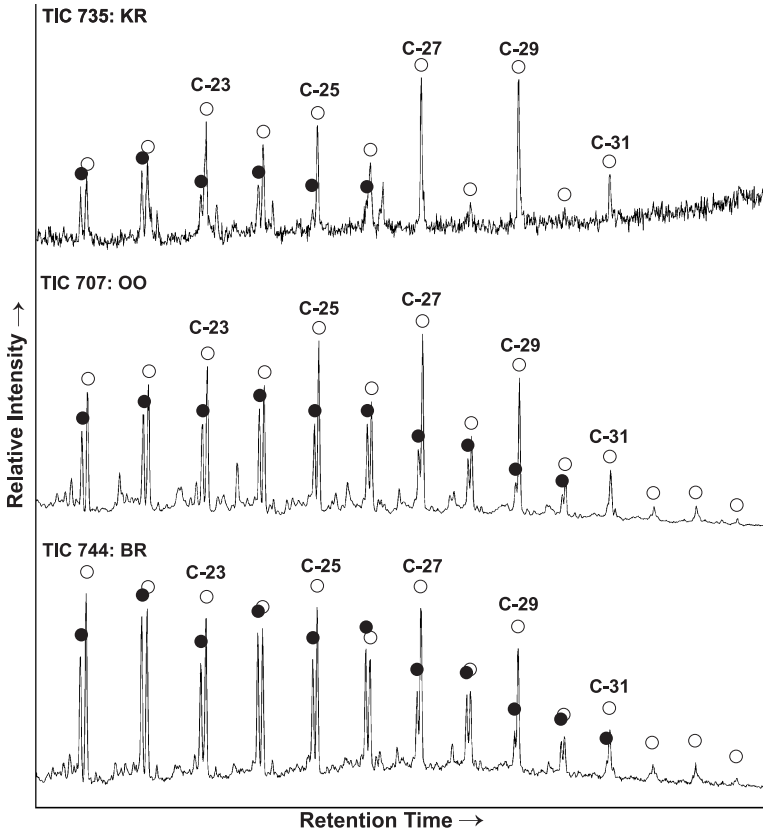


Fig. 4. Long-chain aliphatic composition of SOM. Representative partial summed mass chromatograms for alkenes and alkanes (*m/z* 55+57) of the evaporate/pyrolysate mixtures of SOM samples from the Twente (722), Oosterhout (707) and Breda (744) Formation. ○=alkane, ●=alkene. Numbers above peaks indicate number of carbon atoms.

+1.5‰) excursions from the reference value. Three out of thirteen samples from the Kreftenheye Formation show strongly depleted $\delta^{18}O_{carb}$ values (−6‰) with $\delta^{13}C_{carb}$ values depleted less than 1‰. In addition, five samples from this formation and all three samples from the Twente Formation show strongly depleted $\delta^{18}O_{carb}$ and $\delta^{13}C_{carb}$ values down to −3‰ and −8‰, respectively (Fig. 6). These strongly correlated dual depletions are locally present in sediment samples from the first 15 m below surface and are associated with anomalously high carbonate contents of 5–20 wt.%.

### 4.2. Sediment incubations

Aquifer sediments were selected from core 34C-105 (Fig. 1) for the incubation experiments (Table 2). Sediment samples were incubated for 7.5 days under aerobic conditions to determine the reduction activities of the aquifer sediments and to assess the dominantly reactive reductants (Hartog et al., 2002).

Oxygen consumption rates were relatively steady for each of the sediment incubations throughout the experiments (Fig. 7), and their average oxygen consumption rates are presented in Fig. 8. However, carbon dioxide production suffered from an initial lag phase (<3 days), which was especially notable for sediments with the smaller rate of carbon dioxide production (samples 724 and 729 in Fig. 7). As the initial oxygen consumption rates are unaffected, this apparent lag is subscribed to the initial uptake of $CO_2$ through dissolution, aqueous speciation and carbonate dissolution to establish carbonate equilibrium. After the initial lag phase, all $CO_2$ production rates maintained steady state until the end of the experiment. The $CO_2/O_2$ ratios reported here are

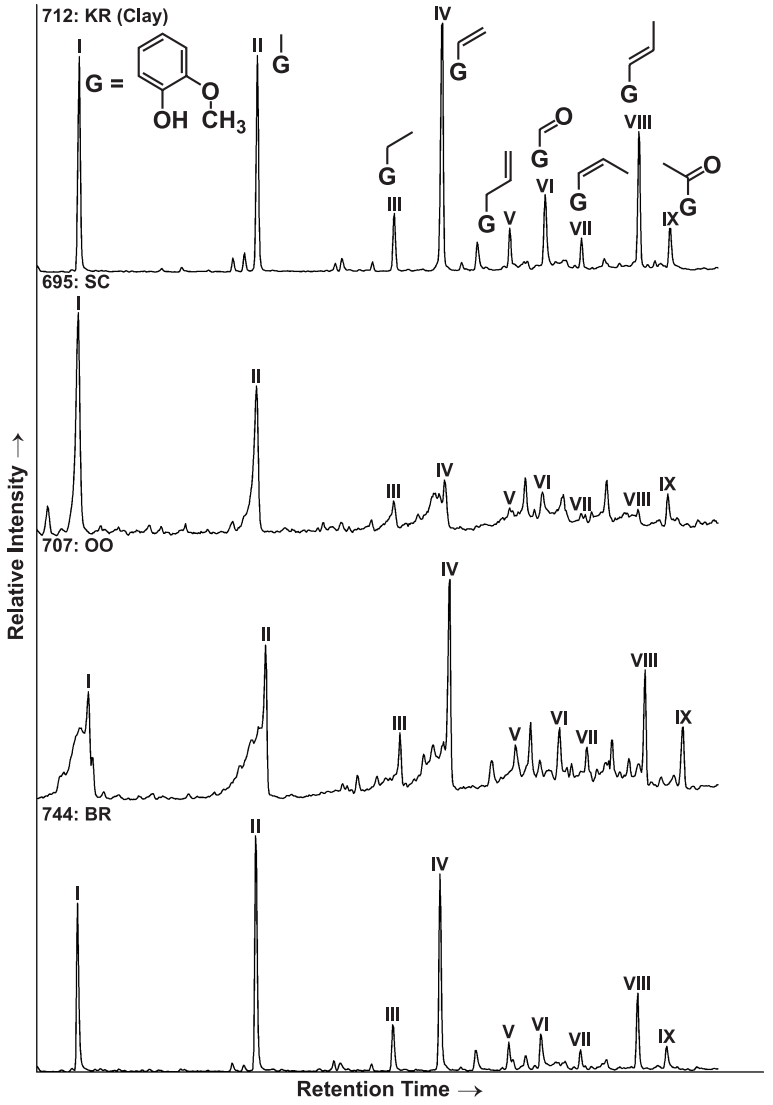


Fig. 5. Lignin composition of SOM. Representative partial summed mass chromatograms for guaiacyl derivatives (*m/z* 124+138+150+152+164+166) of the evaporate/pyrolysate mixtures of SOM from the Kreftenheye Clay (712), Scheemda (695) Oosterhout (707) and Breda (744) samples. Roman numbers in bold refer to the following compounds: **I** Guaiacol (2-methoxyphenol), **II** Methylguaiacol (4-methyl-2-methoxyphenol), **III** Ethylguaiacol (4-ethyl-2-methoxyphenol), **IV** Vinylguaiacol (4-vinyl-2-methoxyphenol), **V** Eugenol (4-(2-propenyl)-2-methoxyphenol), **VI** Vanillin (4-Formyl-2-methoxyphenol), **VII** *cis*-Isoeugenol (*cis*-4-(1-propenyl)-2-methoxyphenol), **VIII** *trans*-Isoeugenol (*trans*-4-(1-propenyl)-2-methoxyphenol), **IX** Acetylguaiacol (4-acetyl-2-methoxyphenol).

those for the final oxygen production and carbon dioxide consumption rates, unaffected by the initial lag phase.

The first two shallow sediments showed high (>0.05 μmol/g day) oxygen consumption rates (Fig. 8B). The lowest rates (<0.02 μmol/g day) were observed for the Kreftenheye sample at 9 m below surface level. Highest rates (up to 0.07 μmol/g day) were observed for the deeper Drente and Oosterhout sediments.

The ratios of $CO_2$ production and $O_2$ consumption were considerably larger than unity (>1.5) for the two shallowest sediments (Fig. 8B) and were associated with high calcium concentrations in the supernatants

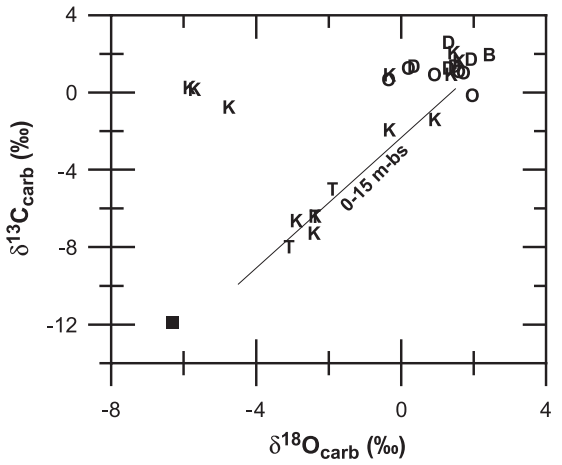


Fig. 6. Cross plot of carbonate isotopic values ($\delta^{18}O_{carb}$ vs. $\delta^{13}C_{carb}$) of the bulk carbonate phase present in the aquifer sediments studied. Codes correspond to samples from the following formations: T=Twente, K=Kreftenheye, D=Drente, O=Oosterhout and B=Breda Formation. Square depicts isotopic signature of dissolved inorganic carbon in present-day groundwater. Line represents the trend due to the diagenetic overprint of groundwater-driven carbonate precipitation.

at the end of the incubations (Table 2). The $CO_2/O_2$ ratio was near unity for the Kreftenheye sample at 9 m below surface level. For the incubation of the deeper sediments, $CO_2/O_2$ ratios ranged from 0.55 to 0.76. Here, an equimolar increase of calcium and sulfate concentrations in the supernatants of the sediments was observed. Final pH values were slightly alkaline in all sediment incubation waters (Table 2). All final incubation waters were saturated (SI~0) with respect to calcite and undersaturated (SI<−0.9) with respect to gypsum (Table 2).

## 5. Discussion

### 5.1. SOM: source and preservation controls

Both molecular and isotopic results point to a terrestrial source for the SOM present in the fluvial and coastal as well as in the marine formations. The observed range of $\delta^{13}C_{org}$ isotopic values (~−25‰) is characteristic for organic matter derived from higher land plants (Tyson, 1995). In addition, the observed long-chain alkanes (Figs. 3 and 4) with an odd-over-even predominance are typical for aliphatics derived from the cuticular waxes of higher plants (Eglinton and Hamilton, 1967). In addition, the dominance of lignin-derived guaiacyl components and aromatics in the evaporate/pyrolysate mixtures (Figs. 3 and 4) reflect the contribution of plant debris (Saiz-Jimenez and De Leeuw, 1986). The terrestrial origin of SOM in the sediments of the Oosterhout and Breda Formation is in line with the dominance of terrestrial SOM in other aquifer sediments of marine origin (Routh et al., 1999; Schulte, 1998).

Pyrolysis studies on recent sedimentary organic matter have revealed the presence of carbohydrate-based polymers such as cellulose (e.g. Fukushima et al., 1987; Zang and Hatcher, 2002). Therefore, the lack of carbohydrate-based pyrolysis products indicates that the higher plant-derived SOM has been degraded at least to some extent in all sediments analyzed. Since lignin is selectively preserved during the early stage of diagenesis (Hatcher et al., 1989), the dominance of guaiacyl units with preserved side-chains in the marine Oosterhout and Breda sand

Table 2
Chemical composition of the incubation waters and the ratio between $CO_2$ produced and $O_2$ consumed after 7.5 days of sediment incubation

| Sample code | Depth (m-bs) | pH | Alkalinity (mmol/l) | Ca[a] (mmol/l) | S[b] (mmol/l) | SI Calcite | SI Gypsum | $CO_2/O_2$ (molar) |
|---|---|---|---|---|---|---|---|---|
| 722 | 3.2 | 7.44 | 2.7 | 3.75 | 0.43 | 0.35 | −1.69 | 1.51 |
| 723 | 5.2 | 7.43 | 2.6 | 3.20 | 0.34 | 0.27 | −1.38 | 1.80 |
| 724 | 9.2 | 7.39 | 2 | 1.25 | 0.36 | −0.24 | −2.08 | 1.10 |
| 725 | 12.2 | 7.51 | 1.8 | 1.55 | 0.36 | −0.08 | −2.01 | 0.65 |
| 726 | 17.1 | 7.42 | 2.8 | NA | NA | | | 0.60 |
| 727 | 24.6 | 7.49 | 3 | NA | NA | | | 0.55 |
| 728 | 29.2 | 7.52 | 2.3 | 2.04 | 1.15 | 0.10 | −1.47 | 0.64 |
| 729 | 35.2 | 7.41 | 2.4 | 3.96 | 2.95 | 0.20 | −0.92 | 0.76 |

NA: not analyzed.
[a] Initial calcium concentration: 1.1 mmol/l.
[b] Initial sulfur concentration: 0.21 mmol/l.

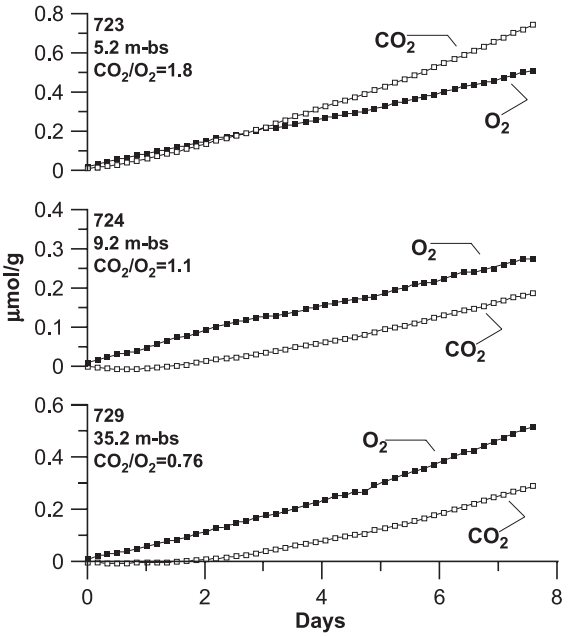


Fig. 7. Evolution of carbon dioxide production and oxygen consumption during incubation of sediments from core: 34C-105. Evolution of oxygen consumption (filled squares) and carbon dioxide production (open squares) in cumulative µmol per g dry sediment during incubation for three selected sediment incubations. Top graph representative for the oxidation of the ferroan carbonate phase present in the two shallowest sediments, middle graph represents the oxidation of SOM in the least reactive sediment, bottom graph represents the oxidation of pyrite and SOM in the deepest, marine Tertiary sediment. The ratios for $CO_2$ production over $O_2$ consumption rates at the end of the experiment are also indicated.

samples (Figs. 3 and 5, Hartog et al., 2004) and the fluvial Kreftenheye clay sample indicates an early stage of SOM degradation. In contrast, the Scheemda sand sample shows a high degree of lignin side-chain oxidation in (695, Fig. 5), similar to the degradation status of SOM in the fluvio-glacially reworked sediments of the Drente Formation (Hartog et al., 2004). The near absence of guaiacol in the Twente (722, Fig. 3) and Kreftenheye sand samples reflect progressed SOM oxidation in these aquifer sediments.

Instead of a dominance by lignin-derived moieties, the samples with more degraded SOM exhibit a pronounced aliphatic signal derived from macromolecular structures (722, Fig. 3), as indicated by the distinct presence of alkanes with important alkene counterparts (Baas et al., 1995; Mosle et al., 1998; Van Smeerdijk and Boon, 1987). This is in line with the observation that macromolecularly bound aliphatics are a relatively stable pool of SOM (Almendros et al., 1996; Leinweber et al., 1996). In addition to the dominance of the macromolecular aliphatic component, the odd-over-even predominance of long-chain *n*-alkanes is more pronounced in the Twente (722, Fig. 3) and Kreftenheye (735, Fig. 4) samples, illustrating the selective preservation of fossil leaf waxes (Logan et al., 1995). Thus, the dominance of the aliphatic signal in these sediment samples reflects the most progressed degradation of SOM.

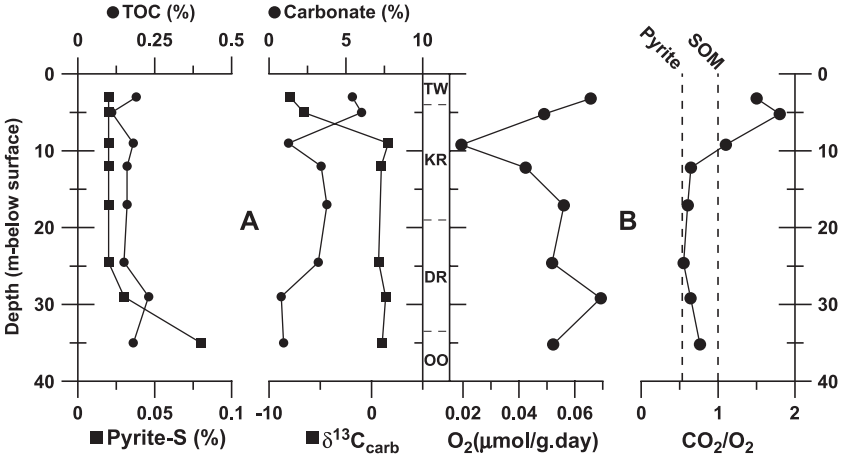


Fig. 8. Bulk chemistry (A) and incubation results (B) of sediments from core 34C-105 (Fig. 1). In (A) TOC, carbonate, and pyrite-S data from van Beek and Vogelaar (1998). In (B) vertical lines represent the molar $CO_2/O_2$ ratios for the oxidation of pyrite (0.533) and SOM (1). Oxidation of ferrous carbonate yields a $CO_2/O_2$ ratio of 4 (Hartog et al., 2002).

As SOM is the principal sorbent of organic contaminants (Pignatello, 1998), the molecular composition of SOM not only controls its degradability, it also affects the sorption capacity of aquifer sediments. The predominance of aliphatic components not only predicts orders of magnitude lower SOM degradability in the sediments with the most degraded SOM (Hartog et al., 2004), but also suggests a higher relative sorption capacity for hydrophobic organic contaminants in these aquifer sediments (Johnson et al., 2001; Salloum et al., 2002; Weber et al., 1998).

Several factors may be responsible for the observed differences in SOM preservation. Clearly, age is an influencing factor, since labile components are degraded preferentially over time. However, SOM from the oldest analyzed Breda Formation (Fig. 2) is relatively well preserved, while SOM from the youngest analyzed Twente and Kreftenheye Formations is more degraded. Therefore, the sediment age difference of 20 My is in itself not a dominant control on the degradation status of SOM in the aquifer sediments studied.

Alternatively, the degree of SOM preservation may reflect differences in oxidation prior to its burial with the sediment. However, the lignin signal in the Kreftenheye clay sample (712, Fig. 5) is remarkably preserved, while lignin-derived components are insignificant in the sandy Kreftenheye (722, Fig. 3) and Twente (722) samples. This suggests that the lower degree of SOM preservation in the Kreftenheye sand (735) is not due to a source effect.

Therefore, the observed range in SOM preservation is most likely generated by differences in deposition and burial conditions, instead of by differences in age or source. Since the observed lignin degradation features are typical for aerobic oxidation (Dijkstra et al., 1998; Dittmar and Lara, 2001; Kuder and Kruge, 1998), the duration that sediments are exposed to oxygen seems to be a controlling factor (Canfield, 1994; Hartnett et al., 1998).

Various factors, such as the oxicity of bottom waters and sedimentation rate, have been linked to the oxygen exposure time (OET) of sediments in marine environments (Canfield, 1994; Gélinas et al., 2001; Hartnett et al., 1998). Gélinas et al. (2001) showed that high sedimentation rates caused shorter OETs for sediments deposited in coastal environments, which led to more preserved SOM when compared with deep-sea sediments, which are exposed to oxygen continuously. Additionally, when oxic degradation is limited by short OETs, the input of labile marine-derived organic matter may help preserve terrestrial SOM in marine depositional environments under oxidant-limited conditions (Hartog et al., 2004).

The aquifer sediments studied originate from a wide range of depositional environments. The steady deposition of sediments in a shallow marine environment (Gélinas et al., 2001; van den Berg et al., 2000) probably resulted in limited OETs, which led to the observed preservation of SOM in the Tertiary Oosterhout and Breda Formations (Figs. 3 and 5). In contrast, the sandy sediments of the Kreftenheye Formation and Twente Formation were deposited in a dominantly braided river system and an ephemeral fluvio-aeolian system, respectively (Van Huissteden and Kasse, 2001; Van Huissteden et al., 2000). The local occurrence of low energetic flow conditions in this overall dynamic environment, allowed the deposition of Kreftenheye clay (Van Huissteden and Kasse, 2001) under less oxygen exposure than its sandy counterpart. This is reflected by the preserved status of SOM in this clay sediment (Fig. 5), which indicates that relatively fresh organic matter was indeed present in this system but that the dynamic conditions under which the sandy sediments are deposited resulted in extensive aerobic SOM degradation. These systems are characterized by repeated sediment remobilization and consequently frequent exposure to atmospheric oxygen. Therefore, the highly dynamic character of these depositional environments likely resulted in long OETs and allowed for extensive degradation of SOM in these sandy aquifer sediments. In addition, OETs increase when sediments are re-exposed to atmospheric conditions such as during the fluvio-glacial reworking of marine Tertiary sediments, which is reflected in the SOM of the Drente sediments being more degraded than in its source sediments (Hartog et al., 2004).

### 5.2. Source of isotopic variation of sedimentary carbonates

The small excursions of less than 2‰ in $\delta^{18}O_{carb}$ and $\delta^{13}C_{carb}$ isotopic values in the Tertiary marine Oosterhout and Breda sediments indicate the syngenetic origin of their carbonate phase (Fig. 6). Synge-

netic carbonate formation during the cold Saalian or Weichselian glacial periods is suggested by the strongly depleted $\delta^{18}O$ and only slightly depleted $\delta^{13}C$ values of the three Kreftenheye samples (Beets and Beets, 2003; Mayer and Schwark, 1999). However, the carbonate phase in other Kreftenheye samples has a marine isotopic signature. As for the Drente carbonate samples in particular, isotopic values plot close to zero with only a slight tendency towards more depleted $\delta^{18}O_{carb}$-values. Since these sediments (Fig. 2) were partly deposited under fluvio-glacial conditions (Saalian), more depleted $\delta^{18}O$-values would be expected for syngenetic carbonates. Therefore, the observed isotopic signature for these samples is at least in part caused by the presence of allogenic marine carbonates. These are likely derived from eroded marine sediments of the Oosterhout or Breda Formations (van den Berg et al., 2000).

A diagenetic overprint is suggested by the strongly depleted $\delta^{13}C_{carb}$-values of the carbonate-enriched shallow Twente and Kreftenheye sediments (Fig. 6). Carbon isotope values of dissolved inorganic carbon (DIC) in present-day groundwater at the site studied are strongly depleted and show an average $\delta^{13}C$-value of −11.9‰ at depth (>10 m-bs) (Van der Grift et al., 2000), indicating that the oxidation of organic matter contributed to DIC (Mook, 1972; Saunders and Swann, 1992). A $\delta^{13}C/\delta^{18}O$ end member for groundwater-derived carbonates (Fig. 6) is derived from the carbon isotope value for DIC and the average $\delta^{18}O$-value of −6.3‰ for present-day precipitation (IAEA, 2000). Moreover, these depleted $\delta^{13}C_{carb}$ and $\delta^{18}O_{carb}$ values compare favorably with the range of those observed for carbonate precipitation in groundwater-fed lake sediments (Kallis et al., 2000; Mayer and Schwark, 1999) and gyttja deposits (Hoek et al., 1999).

### 5.3. Reactivity distribution of observed reductants

The final composition of the incubation waters together with the range of observed ratios of $CO_2$ production to $O_2$ consumption show that various reactive reductants are present in the sediment core studied. The relative importance of these oxidizing reductants varied with depth. During the incubation experiments (Table 2), SOM oxidation was dominant for the Kreftenheye sediment sample 724 (9.2 m-bs) as indicated by the $CO_2/O_2$ ratio close to unity (Table 2, Fig. 8B), according to:

$$C_9H_{10}O_5 + 9O_2 \rightarrow 9CO_2 + 5H_2O.$$

The carbohydrate model of $CH_2O$ is normally used to represent the average composition of SOM. Since the $CO_2/O_2$ for the complete oxidation of organic compounds varies (Hartog et al., 2002), any average representation of SOM should be used with caution unless the oxidation stoichiometries and relative importance of all organic compounds oxidized are known. In the absence of carbohydrate components in the sediments studied, syringate ($C_9H_{10}O_5$) is preferred here as it can be used as a model compound (Chapelle and Bradley, 1996; Hartog et al., 2002) for the observed lignin-derived components (Fig. 5). The resulting $CO_2/O_2$ ratio for the oxidation syringate is similar to that for the partial oxidation of lignin involving the oxidation of its propyl side-chain (Fig. 5).

The relatively unchanged calcium and sulfur concentrations in the final incubation water imply that iron sulfide oxidation was negligible in this sample (Table 2). Therefore, the low oxygen consumption rate of this sample illustrates the low reactivity of SOM in the Kreftenheye Formation, as suggested by its poor preservation. The incubated sediments from greater depth indicated the oxidation of SOM and iron sulfides, as indicated by the $CO_2/O_2$ ratios lower than one and the equimolar increases of calcium and sulfur, according to:

$$FeS_2 + 3¾O_2 + 1½H_2O + 2CaCO_3 \rightarrow Fe(OH)_3 + 2Ca^{2+} + 2SO_4^{2-} + 2CO_2.$$

While pyrite content increases below 25 m-bs (Fig. 8A), the increased $CO_2/O_2$ ratios indicate a decrease in its relative importance of oxygen consumption. In other words, the increased $CO_2/O_2$ ratio suggests that SOM oxidation is more important due to the higher relative reactivity of SOM in the marine Oosterhout sediments. This interpretation is in line with the higher preservation and reactivity of SOM in sediments from the marine Oosterhout Formation lower in the same core when compared with SOM in sediments from the fluvio-glacial Drente Formation (Hartog et al., 2004). A more degraded status of SOM in the Drente sediments may have resulted from

increased oxygen exposure during the reworking of marine sediments, as indicated by their carbonate isotope signatures (Fig. 6). The importance of pyrite oxidation during the incubations of Drente sediments (Fig. 6) leads us to speculate that the reworking of marine sediments had a stronger impact on the reactivity of SOM than on that of pyrite. This suggestion is supported by the observed predominance of pyrite oxidation and the lack of reactive organic matter in aquifer sediments of reworked origin (Postma et al., 1991). A possible explanation for this phenomenon is the formation of a protective iron hydroxide coating on the pyrite surface during reworking under oxic conditions (e.g., Nicholson et al., 1990) after deposition. After re-deposition of the sediment, the reductive dissolution of this coating in groundwater may re-activate the pyrite surface.

The $CO_2/O_2$ ratios higher than 1.5 during the incubation of the two shallowest sediments indicate the oxidation of ferrous iron-bearing calcium carbonate:

$$Fe_{1-x}Ca_xCO_3 + \{1 - x/4\}\cdot O_2 \rightarrow \{1 - x\}\cdot Fe(OH)_3 + x\cdot CaCO_3 + (1 - x)\cdot CO_2 + (1 - x)\cdot H_2O.$$

However, the slightly elevated final calcium concentrations at the end of the incubation (Table 2) and the fact that $CO_2/O_2$ ratios for these samples are lower than expected for the sole oxidation of ferroan calcite (i.e. four), suggest that the $CO_2$ produced was partially consumed by the dissolution of calcium carbonate, following the oxidation of Fe(II)–$CaCO_3$ oxidation under closed conditions (McMillan and Schwertmann, 1998):

$$Fe_{1-x}Ca_xCO_3 + \{1 - x/4\}\cdot O_2 + \{1 + x/2\}\cdot H_2O \rightarrow \{1 - x\}\cdot Fe(OH)_3 + x\cdot Ca^{2+} + 2x\cdot HCO_3^- + (1 - 2x)\cdot CO_2.$$

Alternatively, the aerobic oxidation of $MnCO_3$ results in a $CO_2/O_2$ ratio of 2 and would thus also lead to elevated $CO_2/O_2$ ratios. While the presence of manganous carbonate cannot be excluded, its oxidation is likely unimportant because of the two orders of magnitude lower total manganese contents in sediments as compared with iron (Table 1; van Beek and Vogelaar, 1998). The small increase of sulfur concentrations indicates only a minor contribution by the oxidation of iron sulfides (Table 2).

The resistance to acid attack of part of the carbonate phase that interfered with the $\delta^{13}C_{org}$ determinations is further evidence for the presence of diagenetic carbonates in the two shallowest sediments samples. The refractory nature of Fe(II)-containing carbonates as compared with calcite is well known (Al-Aasm et al., 1990; Jensen et al., 2002; Moore et al., 1992; Morin and Cherry, 1986). Finally, the depleted $\delta^{13}C_{carb}$-values of these samples together with elevated carbonate contents (Fig. 8A) confirm a diagenetic origin (Saunders and Swann, 1992). Therefore, the diagenetic precipitation of a ferrous carbonate phase in these aquifer sediments likely occurred under past alkaline and iron-reducing conditions, as those currently found in deeper groundwater at the site. In contrast with the microbial diagenesis of ferrous carbonates in organic-rich strata (Aslan and Autin, 1996; Postma, 1982, 1983; Taylor, 1998), the exfiltration of deep anoxic groundwater resulting in $CO_2$ degassing may have provided the conditions for the abiotic precipitation of significant amounts of ferrous carbonates (Chae et al., 2001; Hem and Lind, 1994; Hendry, 2002) in these sediments with little reactive organic matter. The observed reactivity of the ferrous carbonate phase is in line with such an origin as (Weber et al., 2001) found chemically precipitated ferrous carbonates to be more prone to oxidation by nitrate than its biogenically formed counterpart.

Based on the presence of highly degraded SOM (Figs. 3 and 5) and insignificant amounts of reduced sulfur (Table 1, Fig. 8A), the initial reduction potential of the Kreftenheye and Twente aquifer sediments is expected to be low. However, paleohydrological conditions may locally have resulted in the precipitation of a Fe(II)-bearing carbonate phase that has resulted in a profound increase of the reduction reactivity of these shallow sediments in the area studied (Fig. 8B).

### 5.4. Controls on the reactivity of sedimentary reductants in groundwater systems

The geochemical composition of sediments varies with provenance, depositional environment and paleohydrological conditions (Galloway and Hobday, 1983; Pettijohn, 1975). Consequently, when assessing

the reduction capacity of aquifer sediments, the presence of a variety of sedimentary reductants has to be considered. In fact, field studies frequently reveal the oxidation of several sedimentary reductants (Böhlke and Denver, 1995; Pauwels et al., 2001). Obviously, the importance of these reductants during sediment oxidation is determined by their relative abundance and reactivity. In the aquifer sediments studied, SOM, pyrite, and Fe(II)-bearing carbonates represent the most reactive phases (Fig. 8). In addition, redox-sensitive glauconitic-Fe(II) (Fanning et al., 1989; Weibel, 1998) may contribute to the reduction capacity of the Pliocene marine Breda sediments (van den Berg et al., 2000), as glauconite weathering presently affects groundwater chemistry in these deposits (Griffioen, 2001).

The overall reactivity of SOM critically depends on the chemical preservation of reactive organic compounds, since labile compounds are degraded preferentially over stable compounds. An order of magnitude difference in SOM reactivity was related to less pronounced side-chain oxidation of lignin-derived components in Oosterhout sediments as compared with Drente sediments (Hartog et al., 2004). Similarly, lignin side-chains are more preserved in SOM from the marine Oosterhout (707) and Breda (744) sediments than in SOM from the coastal Scheemda (695) sediments (Fig. 5), whereas lignin-derived components are depleted in the sandy Kreftenheye and Twente (722, Fig. 3) sediments. Thus, the aquifer sediments studied show a wide range in SOM preservation that predicts degradation rates that differ in orders of magnitude. Therefore, the orders of magnitude range found for in situ SOM oxidation rates in other sedimentary aquifer systems may reflect similar differences in molecular SOM preservation (Chapelle and Lovley, 1990; Jakobsen and Postma, 1994).

The relative preservation of SOM (Fig. 5, Hartog et al., 2004) in the marine Oosterhout sediment coincides with increase of pyrite contents (Fig. 8A). The burial of degradable SOM and the supply of sulfate facilitated diagenetic pyrite formation in this marine sediment. Here, iron and sulfate reduction coupled to the oxidation of relatively preserved SOM resulted in the transfer of sediment reduction capacity from organic carbon to pyrite. Consequently, pyrite is an important reductant in the marine Oosterhout sediments (Fig. 8B). Under carbonate-buffered conditions, the oxidation rate of pyrite is mainly controlled by the amount of reactive surface and impeded by the precipitation of iron hydroxide coatings. Therefore, the reactivity of pyrite decreases with progressive oxidation (Nicholson et al., 1988, 1990). While previous studies have shown that Fe(II)-bearing carbonates in aquifer sediments are potentially reactive towards oxygen and nitrate (Hartog et al., 2002; Weber et al., 2001), the precipitation of iron hydroxide coatings may also decrease the reactivity of ferroan carbonates (Hartog et al., 2002), such as present in the shallow sediments of the Kreftenheye and Twente Formations (Fig. 8).

The relative importance of reductants may change with progressive oxidation as SOM becomes more recalcitrant and reactive mineral reductants are oxidized. In the final stage of aquifer oxidation, when labile SOM components and reactive mineral pools have been oxidized, relatively stable Fe(II)-bearing detrital silicates may represent the main source of reducing activity (Hofstetter et al., 2003; Postma, 1990). Under these conditions, the diffusion of labile organic compounds from adjoining strata rich in preserved SOM, such as clay aquitards (712, Table 1, Fig. 5) or peat layers, may significantly fuel oxidation processes in aquifers (Detmers et al., 2001; McMahon, 2001; McMahon and Chapelle, 1991).

## 6. Conclusions

In variable degrees of importance, the depositional environment of the sediment, the occurrence of subsequent sediment reworking and paleohydrological conditions are all important factors that may affect the relative abundance and reactivity of sedimentary reductants. In the Late Tertiary and Pleistocene sediments that form the aquifer system studied, sedimentary organic matter (SOM), pyrite and ferrous iron contained in carbonates provide the main source of sedimentary reduction capacity. The main findings on what controls the observed distribution and reactivity of each of these reductants are summarized as follows.

While the main source of SOM is higher in land plant derived biomass in all of the sediments studied, the quality of SOM and its anticipated reactivity varies considerably with differences in the depositio-

nal origin of the sediment. SOM is chemically best preserved in aquifer sediments of marine Tertiary origin, as illustrated by the abundance of lignin-derived components with preserved side-chains. In contrast, SOM in the Late Pleistocene fluvial sediments showed the strongest signs of degradation, as demonstrated by insignificant amounts of remaining lignin-derived components and the dominance of recalcitrant macromolecular aliphatic structures. The lower degree of SOM preservation in these sediments is likely due to the higher dynamics of fluvial as compared with marine depositional environments that lead to prolonged exposure to atmospheric oxygen and hence longer and more intense aerobic degradation of SOM.

The increased oxygen exposure by sediment reworking during the Saale ice age was reflected by the more degraded status of SOM in the Pleistocene fluvio-glacial Drente sediments compared to its Tertiary marine source. The availability of relatively preserved SOM in the marine Tertiary sediments most likely facilitated the genesis of pyrite during sulfate reduction after sediment deposition, which resulted in highest pyrite contents found in these sediments. The decreased reactivity of SOM that resulted from sediment reworking was evidenced by the dominance of pyrite oxidation during the incubation of the Drente sediments.

SOM and pyrite do not provide significant reduction capacity in the shallow Pleistocene sediments of fluvial and fluvio-aeolian origin due to their low contents and highly degraded status, respectively. In these sediments however, ferrous iron associated with elevated carbonate contents was locally recognized as a significant reactive reductant during incubation. $\delta^{13}C$ and $\delta^{18}O$ carbonate isotope data suggest that this ferroan carbonate most probably originated from past carbonate precipitation during the exfiltration of Fe(II)-containing anoxic groundwater. This diagenetic overprint resulted in increased reduction activities in the shallow sediments of the aquifer studied.

## Acknowledgements

The authors acknowledge Kees van Beek (Kiwa Research and Consultancy) for providing core samples and bulk geochemical data. The authors are indebted to H.J.J. van Buijsen (TNO Environment, Energy and Process Innovation) for his assistance during the sediment incubations. We wish to thank Drs. C.H. van der Weijden and J.W. de Leeuw for their comments and useful discussions that helped to improve this manuscript. The constructive comments of two anonymous reviewers are appreciated. **[LW]**

## References

Al-Aasm, I.S., Taylor, B.E., South, B., 1990. Stable isotope analysis of multiple carbonate samples using selective acid extraction. Chem. Geol. 80, 119–125.

Almendros, G., Guadalix, M.E., Gonzalez-Vila, F.J., Martin, F., 1996. Preservation of aliphatic macromolecules in soil humins. Org. Geochem. 24 (6–7), 651–659.

Amirbahman, A., Schonenberger, R., Johnson, C.A., Sigg, L., 1998. Aqueous- and solid-phase biogeochemistry of a calcareous aquifer system downgradient from a municipal solid waste landfill (Winterthur, Switzerland). Environ. Sci. Technol. 32 (13), 1933–1940.

Aslan, A., Autin, W.J., 1996. Depositional and pedogenic influences on the environmental geology of Holocene Mississippi River floodplain deposits near Ferriday, Louisiana. Eng. Geol. 45, 417–432.

Baas, M., Briggs, D.E.G., van Heemst, J.D.H., Kear, A.J., de Leeuw, J.W., 1995. Selective preservation of chitin during the decay of shrimp. Geochim. Cosmochim. Acta 59 (5), 945–951.

Barcelona, M.J., Holm, R.T., 1991. Oxidation–reduction capacities of aquifer solids. Environ. Sci. Technol. 25, 1565–1572.

Beets, C.J., Beets, D.J., 2003. A high resolution stable isotope record of the penultimate deglaciation in lake sediments below the city of Amsterdam, The Netherlands. Quat. Sci. Rev. 22 (2–4), 195–207.

Blowes, D., 2002. Environmental chemistry—tracking hexavalent Cr in groundwater. Science 295 (5562), 2024–2025.

Böhlke, J.K., Denver, J.M., 1995. Combined use of groundwater dating, chemical, and isotopic analyses to resolve the history and fate of nitrate contamination in two agricultural watersheds, Atlantic coastal plain, Maryland. Water Resour. Res. 31 (9), 2319–2339.

Bradley, P.M., McMahon, P.B., Chapelle, F.H., 1995. Effects of carbon and nitrate on denitrification in bottom sediments of an effluent-dominated river. Water Resour. Res. 31 (4), 1063–1068.

Bradley, P.M., Chapelle, F.H., Wilson, J.T., 1998. Field and laboratory evidence for intrinsic biodegradation of vinyl chloride contamination in a Fe(III)-reducing aquifer. J. Contam. Hydrol. 31, 111–127.

Canfield, D.E., 1994. Factors influencing organic carbon preservation in marine sediments. Chem. Geol. 114, 315–329.

Chae, G.T., Yun, S.T., Kim, S.R., Hahn, C., 2001. Hydrogeochemistry of seepage water collected within the Youngcheon

diversion tunnel, Korea: source and evolution of $SO_4$-rich groundwater in sedimentary terrain. Hydrol. Process. 15 (9), 1565–1583.

Chapelle, F.H., Bradley, P.M., 1996. Microbial acetogenesis as a source of organic acids in ancient Atlantic Coastal Plain sediments. Geology 24, 925–928.

Chapelle, F.H., Lovley, D.R., 1990. Rates of microbial metabolism in deep coastal plain aquifers. Appl. Environ. Microbiol. 56 (6), 1865–1874.

Desimone, L.A., Howes, B.L., 1996. Denitrification and nitrogen transport in a coastal aquifer receiving wastewater discharge. Environ. Sci. Technol. 30 (4), 1152–1162.

Detmers, J., Schulte, U., Strauss, H., Kuever, J., 2001. Sulfate reduction at a lignite seam: microbial abundance and activity. Microb. Ecol. 42 (3), 238–247.

Dijkstra, E.F., Boon, J.J., van Mourik, J.M., 1998. Analytical pyrolysis of a soil profile under Scots pine. Eur. J. Soil Sci. 49, 295–304.

Dittmar, T., Lara, R.J., 2001. Molecular evidence for lignin degradation in sulfate-reducing mangrove sediments (Amazônia, Brazil). Geochim. Cosmochim. Acta 65 (9), 1417–1428.

Eglinton, G., Hamilton, R.J., 1967. Leaf epicuticular waxes. Science 156 (780), 1322–1335.

Fanning, D.S., Rabenhorst, M.C., May, L., Wagner, D.P., 1989. Oxidation-state of iron in glauconite from oxidized and reduced zones of soil-geologic columns. Clays Clay Miner. 37 (1), 59–64.

Fukushima, K., Yamamoto, S., Uzaki, M., Morinaga, S., Ishiwatari, R., 1987. Characterization of the microbial degradation products of a submerged plant with particular reference to the production of the kerogen-like material. Chem. Geol. 64 (1–2), 169–179.

Funnell, B.M., 1996. Plio-Pleistocene palaeogeography of the Southern North Sea basin (3.75–0.60 Ma). Quat. Sci. Rev. 15 (5–6), 391–405.

Galloway, W.E., Hobday, D.K., 1983. Terrigenous Clastic Depositional Systems: Applications to Petroleum, Coal, and Uranium Exploration. Springer-Verlag, New York. 423 pp.

Gélinas, Y., Baldock, J.A., Hedges, J.I., 2001. Organic carbon composition of marine sediments: effect of oxygen exposure time on oil generation potential. Science 294, 145–148.

Griffioen, J., 2001. Potassium adsorption ratios as an indicator for the fate of agricultural potassium in groundwater. J. Hydrol. 254 (1–4), 244–254.

Hartnett, H.E., Keil, R.G., Hedges, J.I., Devol, A.H., 1998. Influence of oxygen exposure time on organic carbon preservation in continental margin sediments. Nature 391, 572–574.

Hartog, N., Griffioen, J., Van der Weijden, C.H., 2002. Distribution and reactivity of $O_2$-reducing components in sediments from a layered aquifer. Environ. Sci. Technol. 36 (11), 2338–2344.

Hartog, N., Van Bergen, P.F., de Leeuw, J.W., Griffioen, J., 2004. Reactivity of organic matter in aquifer sediments: geological and geochemical controls. Geochim. Cosmochim. Acta 68 (6), 1281–1292.

Hatcher, P.G., Wilson, M.A., Vassallo, A.M., Lerch III, H.E., 1989. Studies of angiospermous wood in Australian brown coal by nuclear magnetic resonance and analytical pyrolysis: new insights into the early coalification process. Int. J. Coal Geol. 13 (1–4), 99–126.

Hem, J.D., Lind, C.J., 1994. Chemistry of manganese precipitation in Pinal Creek, Arizona, USA: a laboratory study. Geochim. Cosmochim. Acta 58 (6), 1601–1613.

Hendry, J.P., 2002. Geochemical trends and palaeohydrological significance of shallow burial calcite and ankerite cements in Middle Jurassic strata on the East Midlands Shelf (onshore UK). Sediment. Geol. 151 (1–2), 149–176.

Heron, G., Christensen, T.H., 1995. Impact of sediment-bound iron on redox buffering in a landfill leachate polluted aquifer (Vejen, Denmark). Environ. Sci. Technol. 29 (1), 187–192.

Hill, A.R., Devito, K.J., Campagnolo, S., Sanmugadas, K., 2000. Subsurface denitrification in a forest riparian zone: interactions between hydrology and supplies of nitrate and organic carbon. Biogeochemistry 51, 193–223.

Hoek, W.Z., Bohncke, S.J.P., Ganssen, G.M., Meijer, T., 1999. Lateglacial environmental changes recorded in calcareous gyttja deposits at Gulickshof, southern Netherlands. Boreas 28 (3), 416–432.

Hofstetter, T.B., Schwarzenbach, R.P., Haderlein, S.B., 2003. Reactivity of Fe(II) species associated with clay minerals. Environ. Sci. Technol. 37 (3), 519–528.

IAEA, 2000. GNIP Database. The International Atomic Energy Agency.

Jakobsen, R., Postma, D., 1994. In situ rates of sulfate reduction in an aquifer (Rømø, Denmark) and implications for the reactivity of organic matter. Geology 22, 1103–1106.

Jakobsen, R., Postma, D., 1999. Redox zoning, rates of sulfate reduction and interactions with Fe-reduction and methanogenesis in a shallow sandy aquifer, Rømø, Denmark. Geochim. Cosmochim. Acta 63 (1), 137–151.

Jensen, D.L., Boddum, J.K., Tjell, J.C., Christensen, T.H., 2002. The solubility of rhodochrosite ($MnCO_3$) and siderite ($FeCO_3$) in anaerobic aquatic environments. Appl. Geochem. 17 (4), 503–511.

Johnson, M.D., Huang, W.H., Weber, W.J., 2001. A distributed reactivity model for sorption by soils and sediments: 13. Simulated diagenesis of natural sediment organic matter and its impact on sorption/desorption equilibria. Environ. Sci. Technol. 35 (8), 1680–1687.

Kallis, P., Bleich, K.E., Stahr, K., 2000. Micromorphological and geochemical characterization of Tertiary 'freshwater carbonates' locally preserved north of the edge of Miocen Molasse Basin (SW Germany). Catena 41, 19–42.

Kelly, W.R., 1997. Heterogeneties in ground-water geochemistry in a sand aquifer beneath an irrigated field. J. Hydrol. 198, 154–176.

Kuder, T., Kruge, M.A., 1998. Preservation of biomolecules in subfossil plants from raised peat bogs—a potential paleoenvironmental proxy. Org. Geochem. 29 (5–7), 1355–1368.

Lee, W., Batchelor, B., 2003. Reductive capacity of natural reductants. Environ. Sci. Technol. 37 (3), 535–541.

Leinweber, P., Jordan, E., Schulten, H.R., 1996. Molecular characterization of soil organic matter in Pleistocene moraines from the Bolivian Andes. Geoderma 72 (1–2), 133–148.

Logan, G.A., Smiley, C.J., Eglinton, G., 1995. Preservation of fossil leaf waxes in association with their source tissues,

Clarkia, northern Idaho, USA. Geochim. Cosmochim. Acta 59 (4), 751–763.

Lovley, D.R., Chapelle, F.H., Phillips, E.J.P., 1990. Fe(III)-reducing bacteria in deeply buried sediments of the Atlantic coastal-plain. Geology 18 (10), 954–957.

Magaritz, M., Luzier, J.E., 1985. Water–rock interactions and seawater–freshwater mixing effects in the coastal dunes aquifer, Coos Bay, Oregon. Geochim. Cosmochim. Acta 49, 2515–2525.

Mayer, B., Schwark, L., 1999. A 15,000-year stable isotope record from sediments of Lake Steisslingen, Southwest Germany. Chem. Geol. 161, 315–337.

McMahon, P.B., 2001. Aquifer/aquitard interfaces: mixing zones that enhance biogeochemical reactions. Hydrogeol. J. 9 (1), 34–43.

McMahon, P.B., Chapelle, F.H., 1991. Microbial production of organic acids in aquitard sediments and its role in aquifer geochemistry. Nature 349, 233–235.

McMillan, S.G., Schwertmann, U., 1998. Morphological and genetic relations between siderite, calcite and goethite in a Low Moor Peat from southern Germany. Eur. J. Soil Sci. 49, 283–293.

Molenat, J., Durand, P., Gascuel-Odoux, C., Davy, P., Gruau, G., 2002. Mechanisms of nitrate transfer from soil to stream in an agricultural watershed of French Brittany. Water Air Soil Pollut. 133 (1–4), 161–183.

Mook, W.G., 1972. Application of natural isotopes in ground water hydrology. Geol. Mijnb. 51 (1), 131–136.

Moore, S.E., Ferrell, R.E., Aharon, P., 1992. Diagenetic siderite and other ferroan carbonates in a modern subsiding marsh sequence. J. Sediment. Petrol. 62 (3), 357–366.

Morin, K.A., Cherry, J.A., 1986. Trace amounts of siderite near a uranium-tailings impoundment, Elliot Lake, Ontario, Canada, and its implication in controlling contaminant migration in a sand aquifer. Chem. Geol. 56 (1–2), 117–134.

Morris, J.T., Whiting, G.J., Chapelle, F.H., 1988. Potential denitrification rates in deep sediments from the southeastern coastal plain. Environ. Sci. Technol. 22 (7), 832–836.

Mosle, B., et al., 1998. Factors influencing the preservation of plant cuticles: a comparison of morphology and chemical composition of modern and fossil examples. Org. Geochem. 29 (5–7), 1369–1380.

Nicholson, R.V., Gillham, R.W., Reardon, E.J., 1988. Pyrite oxidation in carbonate-buffered solution: 1. Experimental kinetics. Geochim. Cosmochim. Acta 52, 1077–1085.

Nicholson, R.V., Gillham, R.W., Reardon, E.J., 1990. Pyrite oxidation in carbonate-buffered solution: 2. Rate control by oxide coatings. Geochim. Cosmochim. Acta 54, 395–402.

Parkhurst, D.L., Appelo, C.A.J., 1999. User's guide to PHREEQC (Version 2). Water Resources Investigations Report 99-4295. U.S. Geological Survey, Denver Colorado.

Pauwels, H., Lachassagne, P., Bordenave, P., Foucher, J.C., Martelat, A., 2001. Temporal variability of nitrate concentrations in a schist aquifer and transfer to surface waters. Appl. Geochem. 16, 583–596.

Pedersen, J.K., Bjerg, P.L., Christensen, T.H., 1991. Correlation of nitrate profiles with groundwater and sediment characteristics in a shallow sandy aquifer. J. Hydrol. 124, 263–277.

Pettijohn, F.J., 1975. Sedimentary Rocks. Harper and Row, New York. 628 pp.

Pfenning, K.S., McMahon, P.B., 1996. Effect of nitrate, organic carbon, and temperature on potential denitrification rates in nitrate-rich riverbed sediments. J. Hydrol. 187, 283–295.

Pignatello, J.J., 1998. Soil organic matter as a nanoporous sorbent of organic pollutants. Adv. Colloid Interface Sci. 76–77, 445–467.

Postma, D., 1982. Pyrite and siderite formation in brackish and freshwater swamp sediments. Am. J. Sci. 282, 1151–1183.

Postma, D., 1983. Pyrite and siderite oxidation in swamp sediments. J. Soil Sci. 34, 163–182.

Postma, D., 1990. Kinetics of nitrate reduction by detrital Fe(II)-silicates. Geochim. Cosmochim. Acta 54 (3), 903–908.

Postma, D., Boesen, C., Kristiansen, H., Larsen, F., 1991. Nitrate reduction in an unconfined sandy aquifer: water chemistry, reduction processes, and geochemical modeling. Water Resour. Res. 27 (8), 2027–2045.

Puckett, L.J., Cowdery, T.K., 2002. Transport and fate of nitrate in a glacial outwash aquifer in relation to ground water age, land use practices, and redox processes. J. Environ. Qual. 31 (3), 782–796.

Routh, J., McDonald, T.J., Grossman, E.L., 1999. Sedimentary organic matter sources and depositional environment in the Yegua formation (Brazos County, Texas). Org. Geochem. 30 (11), 1437–1453.

Saiz-Jimenez, C., De Leeuw, J.W., 1986. Chemical characterization of soil organic matter fractions by analytical pyrolysis-gas chromatography–mass spectrometry. J. Anal. Appl. Pyrolysis 9 (2), 99–119.

Salloum, M.J., Chefetz, B., Hatcher, P.G., 2002. Phenanthrene sorption by aliphatic-rich natural organic matter. Environ. Sci. Technol. 36 (9), 1953–1958.

Sanchez-Monedero, M.A., Roig, A., Cegarra, J., Bernal, M.P., Paredes, C., 2002. Effects of HCl-HF purification treatment on chemical composition and structure of humic acids. Eur. J. Soil Sci. 53 (3), 375–381.

Saunders, J.A., Swann, C.T., 1992. Nature and origin of authigenic rhodochrosite and siderite from the Paleozoic aquifer, northeast Mississippi, USA. Appl. Geochem. 7 (4), 375–387.

Schmidt, M.W.I., Knicker, H., Hatcher, P.G., KogelKnabner, I., 1997. Improvement of C-13 and N-15 CPMAS NMR spectra of bulk soils, particle size fractions and organic material by treatment with 10% hydrofluoric acid. Eur. J. Soil Sci. 48 (2), 319–328.

Schulte, U., 1998. Isotopengeochemische Untersuchungen zur Charakterisierung biologisch geteuerter Redoxprozesse in Aquiferen der Niederrheinischen Bucht. Ruhr-Universität Bochum, Bochum. 169 pp.

Smith, R.L., Duff, J.H., 1988. Denitrification in a sand and gravel aquifer. Appl. Environ. Microbiol. 54 (5), 1071–1078.

Starr, J.L., Sadeghi, A.M., Parkin, T.B., 1996. A tracer test to determine the fate of nitrate in shallow groundwater. J. Environ. Qual. 25, 917–923.

Taylor, K.G., 1998. Spatial and temporal variations in early diagenetic organic matter oxidation pathways in Lower Jurassic mudstones of eastern England. Chem. Geol. 145, 47–60.

Tyson, R.V., 1995. Sedimentary Organic Matter. Chapman & Hall, London. 615 pp.

Uffink, G.J.M., Römkens, P.F.A.M., 2001. Nitrate transport modeling in deep aquifers. Comparison between model results and data from the groundwater monitoring network. 711401010, National Institute of Public Health and the Environment (RIVM), Bilthoven, The Netherlands.

van Beek, C.G.E.M., Vogelaar, A.J., 1998. Pompstation Hengelo 't Klooster—Geohydrologische, geochemische en hydrochemische beschrijving. KOA 98.100, KIWA N.V., Nieuwegein, The Netherlands.

van den Berg, M.W., van Houten, C.J., den Otter, C., 2000. Geologische Kaart van Nederland, Blad Enschede West (34W) en Enschede Oost/Glanerbrug (34O/35). Nederlands Instituut voor Toegepaste Geowetenschappen TNO, Utrecht.

Van der Grift, B., Minnema, B., Griffioen, J., 2000. Een geintegreerd transportmodel voor grondwaterkwaliteit. Deelrapport 14. Test op freatische winning 't Klooster, Gelderland. NITG 00-134-B, NITG-TNO, KIWA, Utrecht, The Netherlands.

Van Huissteden, J.K., Kasse, C., 2001. Detection of rapid climate change in Last Glacial fluvial successions in The Netherlands. Glob. Planet. Change 28, 319–339.

Van Huissteden, J.K., Vandenberghe, J., Van der Hammen, T., Laan, W., 2000. Fluvial and aeolian interaction under permafrost conditions: Weichselian Late Pleniglacial, Twente, eastern Netherlands. CATENA 40 (3), 307–321.

Van Smeerdijk, D.G., Boon, J.J., 1987. Characterisation of subfossil Sphagnum leaves, rootlets of ericaceae and their peat by pyrolysis-high-resolution gas chromatography–mass spectrometry. J. Anal. Appl. Pyrolysis 11, 377–402.

Weber Jr., W.J., Huang, W., Yu, H., 1998. Hysteresis in the sorption and desorption of hydrophobic organic contaminants by soils and sediments: 2. Effects of soil organic matter heterogeneity. J. Contam. Hydrol. 31 (1–2), 149–165.

Weber, K.A., Picardal, F.W., Roden, E.E., 2001. Microbially catalyzed nitrate-dependant oxidation of biogenic solid-phase Fe(II) compounds. Environ. Sci. Technol. 35, 1644–1650.

Weibel, R., 1998. Diagenesis in oxidising and locally reducing conditions—an example from the Triassic Skagerrak formation, Denmark. Sediment. Geol. 121 (3–4), 259–276.

Zang, X., Hatcher, P.G., 2002. A Py–GC–MS and NMR spectroscopy study of organic nitrogen in Mangrove Lake sediments. Org. Geochem. 33 (3), 201–211.